ELSEVIER

Thermochimica Acta 347 (2000) 45–51

thermochimica acta

www.elsevier.com/locate/tca

Investigations of the temperature gradients affecting the temperature scale of a 3ω-heat capacity spectrometer

Ulf G. Jonsson[a,*], Ove Andersson[b], Åke Fransson[a]

[a]*Umeå University, Applied Physics and Electronics, S-90187 Umeå, Sweden*
[b]*Umeå University, Department of Experimental Physics, S-90187 Umeå, Sweden*

Received 1 October 1999; accepted 7 October 1999

Abstract

The temperature gradients affecting the temperature scale of a dynamic heat capacity spectrometer based on the 3ω-method are investigated using the SmecticA-Nematic (SmA/N) transition in the liquid crystal octyloxycyanobiphenyl (8OCB). The heater (sample) temperature was obtained from a thermocouple by superimposing the temperature increase of the heater, where the increase was calculated from the heater power. The calibration using the SmA/N transition yields a linear relation between the temperature rise of the heater ΔT_h and the heater power P: $\Delta T_h = 55.2P$. An estimation of the maximum temperature gradient in the 8OCB sample shows that the correction of the sample temperature due to the gradient is small compared to ΔT_h (<-0.01 K for $\omega = 3.98.\ 2\pi$ rads^{-1} and -0.14 K for $\omega = 0.01.\ 2\pi$ rads^{-1}). For high heating powers there is a significant temperature gradient in the heater, which causes a broadening of the SmA/N peakwidth from 0.5 K for $P = 7.7$ mW to 2 K for $P = 29.4$ mW.

Keywords: 3ω-heat capacity spectrometer; 3ω-method, temperature calibration; 8OCB

1. Introduction

In 1985 Birge and Nagel [1] introduced heat capacity spectroscopy in which the sample is probed using a sinusoidally varying temperature. In this case, one obtains the product of the thermal conductivity κ, and the dynamic specific heat capacity per unit volume c_p, of a sample. That is, the specific heat can be divided in real and imaginary components, which are associated with molecular motions that are in and out of phase with the temperature oscillation of the probe, respectively. In order to measure dynamic specific heat, Birge and Nagel [2] used a method which is generally referred to as the 3ω-method.

The 3ω-method for measuring dynamic heat capacity is based on the principle of using a thin (ca. 0.1 μm) metallic strip as both heater and thermometer. A sinusoidally varying current of frequency ω is supplied to the heater which is located on the surface of the sample. For a liquid sample, the heater is placed on a substrate which is submerged in the liquid. The combination of strip and substrate form the 3ω-sensor. The electrical power input to the heater consists of dc- and ac-components, where the latter dissipates through thermal waves of frequency 2ω that diffuses into the sample. A measured ac-voltage over the heater gives an amplitude modulated signal with components at frequency ω and 3ω. The amplitude of the signal at

* Corresponding author. Fax: +46-90-7866469.
E-mail address: ulf.jonsson@tfe.umu.se (U.G. Jonsson).

0040-6031/00/$ – see front matter
PII: S0040-6031(99)00415-3

3ω yields the temperature oscillation of the heater, which depends on the thermal properties of the sample.

The ideal planar heater model [3] assumes an infinitely thin heater with a constant amplitude of the temperature oscillation throughout its whole area. The alternating electric current in the heater also leads to a dc-heating that causes a temperature rise ΔT_h, of the heater above the ambient temperature T_{amp}. Therefore, for high heater power a significant temperature difference ΔT_{grad}, arises along the heater. As a consequence, the peak in the heat capacity associated with a transition will be broadened. Furthermore, the dc-heating creates a temperature gradient in the sample. This affects the sample temperature and, therefore, transition temperatures. The SmecticA-Nematic (SmA/N) transition in the liquid crystal octyloxycyanobiphenyl (8OCB) has been studied to understand how the design of the heater and the construction of the sample cell influences the temperature scale and the width of a transition peak.

2. Experimental method

A schematic figure of the sample cell is shown in Fig. 1. The sensor is placed between two 50 mm diameter, 15 mm thick, aluminium cylinders. Both the cylinders have wire heaters mounted on their circumferences. The temperature controller (see following paragraph) uses the wire-heaters to keep the sample at constant temperature while measuring. A thermocouple of type K (Chromel-Alumel), designated T2, is mounted between the substrate and the

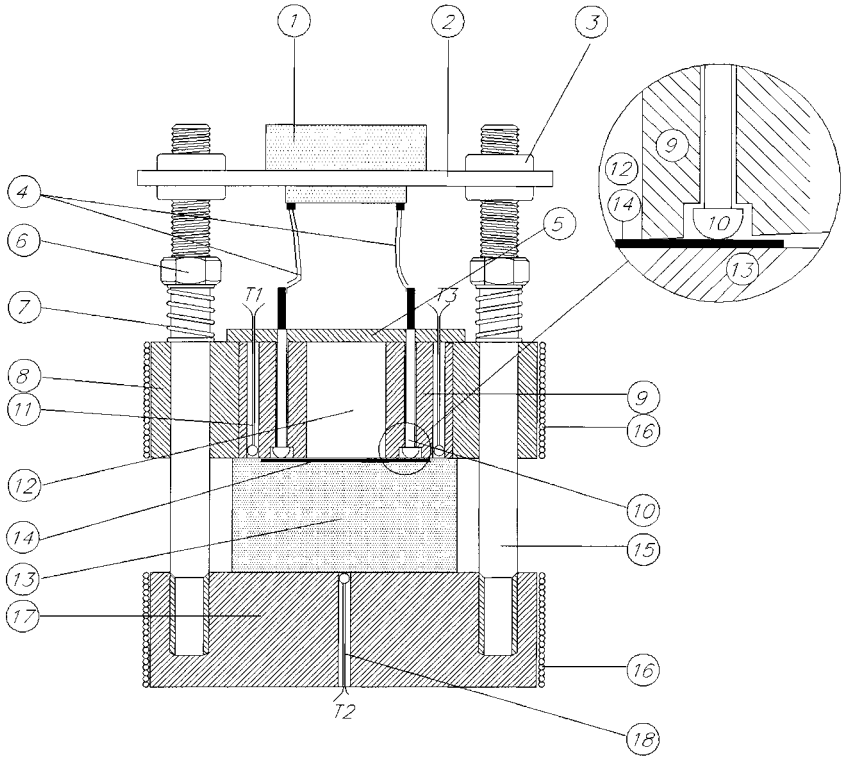

Fig. 1. Cross-section of the measuring cell. The magnified part shows the wedge shaped form of the lower end of the Teflon sample cell. 1-electrical multipole contact, 2-fiber glass board, 3-nut made of Teflon, act as a holder of the fiber glass board, 4-electrical wires, 5-lid of aluminium, 6-steel nut, 7-spring, 8-aluminium top section, 9-Teflon sample cell, 10-electrical spring loaded contact, 11-thermocouple, 12-sample volume, 13-glass substrate, 14-Nickel heater, 15-steel threaded bolt, 16-wire wound heater, 17-aluminium lower section, 18-temperature controller sensing thermocouple.

lower cylinder. Temperature measured by T2 is used as input to the controller. The upper cylinder holds the cylindrical sample cell made of Teflon. The end of the Teflon cylinder in contact with the substrate has a small wedge to ensure a construction free from leakage. Thermocouples T1 and T3 (type K) are mounted between the lower end of the Teflon cylinder and the substrate. The sample temperature is obtained by adding the temperature increase of the heater to the average of T1 and T3 (see the discussion in the paragraph below about the influence on the sample temperature of the temperature gradient in the sample). The thermocouples were calibrated using a HP 2804/18111A quartz thermometer, traceable to IPTS-68, with an absolute accuracy of +/−0.040 K.

The substrate, supporting the heater, is made of window-glass of thickness 15 mm [3]. The nickel heater is evaporated onto the substrate. The heater is I-shaped (20×2 mm^2) and with 6×2 mm^2 contact pads at the ends. The heater thickness is 0.1 μm, which is monitored by a film thickness monitor using a quartz crystal oscillator during the deposition process. The heater is electrically contacted in a four probe fashion by spring loaded contacts, 1 mm in diameter, mounted vertically in the wall of the Teflon cylinder. To ensure good electrical contact, a silver layer with a thin gold layer on top is deposited onto each contact pad. The resistance of the heater is about 10 Ω. The cell can be hermetically sealed by a metallic lid on top of the Teflon cylinder. After the sample is inserted in the cell, argon gas is added through small 1 mm-pipe fittings in the lid.

To suppress the large fundamental signal at frequency ω, the heater is mounted in a bridge as shown in Fig. 2. The bridge driving voltage, Vb, comes from an external power amplifier connected to the internal oscillator of a Stanford Research Systems model SR830 programmable lock-in amplifier. The two resistances, Rb, form a voltage divider. Rs is a resistance in series with the heater resistance that can be varied by the bridge balancing unit. Both Rb and Rs are made of manganin which has an almost temperature independent resistance. R0 is the heater resistance. C_v is a small variable capacitance (ca. 4 *nF*) which is used to balance the bridge at frequencies where the heater also has a small capacitive contribution which affects the bridge balance. A careful wiring of the bridge circuit is essential as cable capacitances easily affect the behaviour of the bridge. The key to a successful design is to keep always the symmetry situation of the bridge. In our design we have used same type, equally long, coaxial cables for all connections of signal paths. As the input resistance of the bridge is about 5 Ω, the power amplifier has an output resistance of equal value for maximum power transfer to the heater. The lock-in amplifier can be set to lock at frequency multiples of the oscillator frequency and in this case the third harmonic is selected. A Keithley 2000 digital voltmeter is used to measure the electrical power input to the heater.

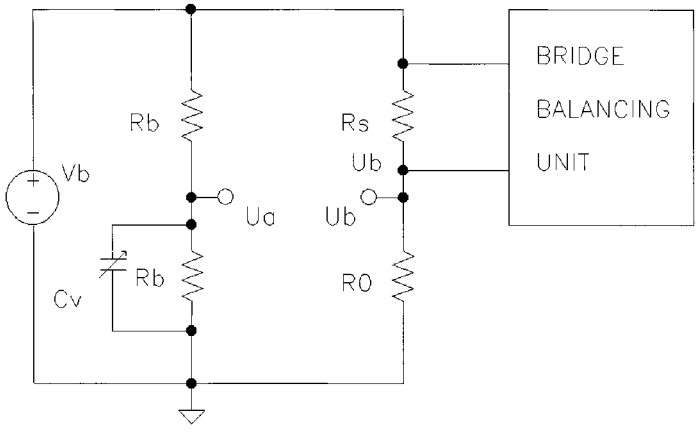

Fig. 2. Generalised circuit diagram of the Wheatstone bridge with the automatic bridge balancing unit.

The sample cell is enclosed in a coaxial dual-Dewar vessel system where the space between the outer and inner Dewar is filled with ice-water mixture for cooling. A temperature controller, Omron EC5 K, regulates the temperature of the sample within 20 mK. The controller is fully programmable and is used to step the sample temperature while measuring the 3ω-voltage.

For every measured point a number of criteria must be met. In short, the measuring algorithm is as follows. At the start of the experiment, the heater power is set to a fixed value in the range of 200–1000 Wm^{-2}. The sample temperature is increased in small discrete steps, normally in the range 50–200 mK. After each step, the temperature is kept constant until equilibrium conditions are established. A 5-sample running average of the heater resistance is computed with a 1 min interval between each sample. Every sample includes a zeroing cycle of the bridge. The system is considered in equilibrium if the standard deviation of the 5-sample buffer is less than 0.1%, which corresponds to a variation in temperature of 20 mK during the 5 min period. When this equilibrium criterion is met the heater power is measured. If the power is not within 0.1% of the fixed value, due to variation of the heater resistance with temperature, then the heater power is adjusted and a new equilibrium cycle is initiated. If both the equilibrium and the power criteria are met, the 3ω-voltage is measured. The measuring rate is about 0.1 K/h using steps of 20 mK.

The measuring system is controlled via an IEEE-488 instrument bus connected between a personal computer, the lock-in amplifier and the digital voltmeter. The temperature controller, EC5 K, is programmed via a RS-232 serial link. The EC5K has its own processor which means that it can operate without interrupting the PC. The automatic bridge zeroing unit is directly connected to the PC through a 16 bit digital I/O-card.

The product $\kappa\, c_\mathrm{p}$ of the sample and substrate are related to the oscillating heater temperature, T_0, by the following equation.

$$T_0 = \frac{J_\mathrm{q}}{\sqrt{2\omega(\kappa c_\mathrm{p})_\mathrm{su}} + \sqrt{2\omega(\kappa c_\mathrm{p})_\mathrm{sa}}} \mathrm{e}^{-\mathrm{i}(\pi/4)} \qquad (1)$$

where J_q = electrical power/heater area is the heat flow. Subscripts su and sa refer to substrate and sample, respectively. Eq. (1) is derived under the assumption that the heater is thin and that the heatflow is one-dimensional (ideal planar heater model) [3].

The bridge resistance in series with the nickel heater is adjusted to the same value as the heater resistance by the bridge autozeroing device. This leads to the following expression for the oscillating heater temperature, $T_0 = 2U_{3\omega}/\alpha U_0$ where $U_{3\omega}$ is the heater voltage at frequency 3ω, U_0 is the heater voltage at frequency ω and $\alpha \approx 2\times10^{-3}\ \mathrm{K}^{-1}$ is the temperature coefficient of the heater resistance. Since the temperature coefficient differs slightly between depositions on substrates, it is necessary to determine the value for each sensor [4].

The liquid crystal octyloxycyanobiphenyl (8OCB) [5] was received from Merck KgaA, 64271 Darmstadt, Germany and used without further purification. The SmA/N transition in 8OCB has very small transition enthalpy, of a few J mol^{-1} [6], and the transition does not exhibit supercooling [7]. This is ideal for calibration of the temperature scale since the transition is not disturbed by high transition enthalpy as in the case of the nematic-isotropic (N-I) transition. The sample cell was loaded with approximately 1 cm^3 of 8OCB. Before each series of sweeps over the SmA/N transition, the sample was heated well above the N-I transition at 353 K [8] and kept at this temperature several hours before measuring.

3. Results and discussion

To calculate $(\kappa\, c_\mathrm{p})_\mathrm{sa}$ from Eq. (1), the substrate contribution $(\kappa\, c_\mathrm{p})_\mathrm{su}$ must be subtracted. The cell without a sample was measured at 79 temperatures in the interval 290–370 K and the result was fitted to the function:

$$(\kappa\, c_\mathrm{p})_\mathrm{su} = 2.03\times10^{6}(1 + 3.3\times10^{-3}(T - 298)) \\ \mathrm{J}^2\,\mathrm{s}^{-1}\,\mathrm{m}^{-4}\,\mathrm{K}^{-2}, \quad 290 \le T \le 370\,\mathrm{K} \qquad (2)$$

with a standard deviation of 1.6×10^4 J s^{-1} m^{-4} K^{-2}. The uncertainty in the $\kappa\, c_\mathrm{p}$ measurements is estimated to 5%. Eq. (2) together with Eq. (1) yields $\kappa\, c_\mathrm{p}$ for the sample (8OCB).

Four sweeps with different electrical power were carried out to investigate the effects of the heater temperature rise ΔT_h, the temperature gradient in the sample as well as the gradient in the heater, caused by the dc-heating. In Fig. 3 the product $\kappa\, c_\mathrm{p}$ is plotted

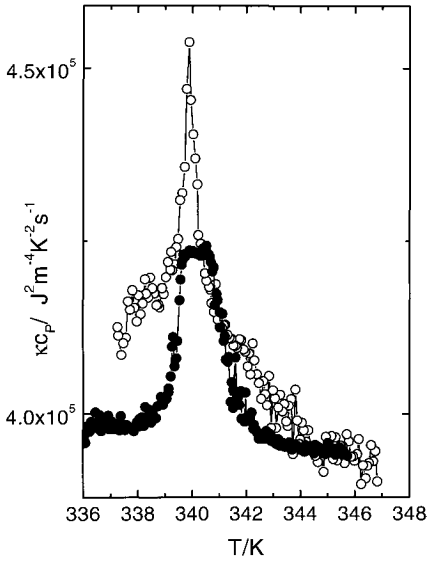

Fig. 3. The SmA/N transition in 8OCB plotted for two different values of heatflow. The temperature scale is corrected for the effect of the temperature gradients. The Φ_{hi}=1090 Wm^{-2} curve is broadened and has a lower peak relative to the Φ_{lo}=287 Wm^{-2} curve due to a larger temperature gradient in the heater.

as a function of temperature for the lowest, Φ_{lo}=287 Wm^{-2}, and highest, Φ_{hi}=1090 Wm^{-2}, heatflow values. The results were obtained at a frequency of 3.98 Hz with 7.7 (Φ_{lo}) and 29.4 mW (Φ_{hi}) electrical power, respectively. Results at increasing temperatures are identical to those at decreasing temperatures. The rms amplitude of the heater temperature is about 13 mK for the lowest heatflow situation.

For low values of the electrical power (input to the heater), the temperature rise caused by the dc-heating is small and, consequently the gradient in the heater will be small. If the heater power is increased, the temperature rise of the heater and the gradient in the heater will also increase, which will influence the temperature scale. It is reasonable to assume that the area in the middle of the heater gets hotter than the peripheral parts where the electrical contacts are placed, and that the temperature difference should be largest for the highest heating power. The Teflon cylinder and the metallic contacts contribute to the formation of the temperature gradient by conducting heat away from the heater. As a consequence, a temperature gradient, mainly along the heater, will arise.

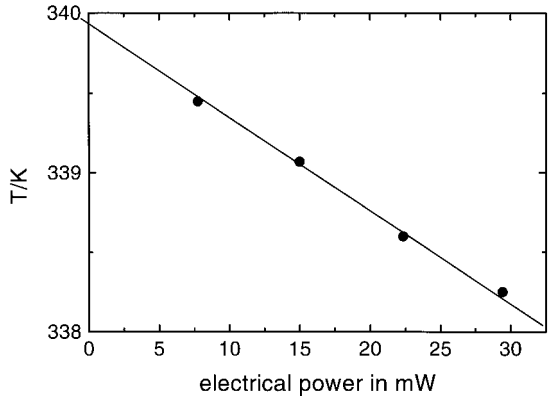

Fig. 4. The SmA/N transition temperature in 8OCB plotted as a function of electrical power input to the heater. A straight line fit yields a value for the zero power transition temperature, T_c=339.90±0.09 K.

Previous results for the SmA/N transition temperature are based on the maximum of the peak in c_p. To compare with these, we should determine the temperature of the maxima in $\kappa\, c_p$ for the different heating powers. If a temperature difference ΔT_{grad} exists in the heater then, at increasing temperature, the part of the heater which has the highest temperature will sense the SmA/N transition first, and the coldest part will sense the transition at a temperature ΔT_{grad} higher. This makes the transition significantly broader for the highest heatflows and it is difficult to determine the temperature for the maximum in $\kappa\, c_p$. Therefore, the onset temperatures for the transition were used to determine the transition temperatures. The peak for $\kappa c_p|^{\Phi_{lo}}$, where ΔT_{grad} should be small, was used to obtain the peak-width of the transition. Half of the peakwidth was added to the onset temperatures to obtain transition temperatures.

As shown in Fig. 4, there is a linear relationship between the power and the transition temperature. From Fig. 4, T_c=339.0±0.09 K was obtained by extrapolation to zero power, which is in good agreement with earlier results for the SmA/N transition temperature [5,6,9]. Zywocinski et al. [8] measured the transition temperature to 339.99 K using a platinum resistance thermometer calibrated on ITPS-68 (which corresponds to 339.97 K on the ITS-90 scale). For this sensor, a coefficient of 55.2 KW^{-1} multiplied by the heater power yields the temperature rise of the heater.

In addition to the temperature of the heater, the calibration accounts for the temperature gradient in the sample $\Delta T_{sa}/\Delta x$, where x is normal to the plane of the heater. This part depends on the probe frequency, but as shown below it is small in comparison with ΔT_h. A thermal wave diffuses into the sample with a characteristic thermal penetration depth $\lambda = \sqrt{D/\omega}$, where D is the diffusivity of the sample and ω is the frequency of the electric current. The sample must be thick enough so that the major part of the thermal wave is enclosed in the sample, or else a two-layer situation arises which will affect the measured amplitude T_0. To avoid boundary effects, a sufficient sample thickness should be more than 7λ [3], then the amplitude of the temperature oscillation is less than 0.1% of the heater temperature oscillation. Since the penetration depth changes with frequency, this will effect the temperature calibration. The temperature which corresponds to the measured value for $\kappa\, c_p$ should be an average of the sample temperature. The amplitude of the temperature oscillation decreases exponentially with $\lambda\,(\propto T_0 e^{-(x/\lambda)})$. An estimate would be to use the temperature obtained by:

$$\langle T_{sa}\rangle = \frac{\int_0^{7\lambda} T(x) e^{-(x/\lambda)} dx}{\int_0^{7\lambda} e^{-(x/\lambda)} dx} \quad (3)$$

where $T(x)=T_{amb}+\Delta T_h+(\Delta T_{sa}/\Delta x)x$. Evaluation of Eq. (3) yields the sample temperature as:

$$\langle T_{sa}\rangle = T_{amb} + \Delta T_h + \frac{\Delta T_{sa}}{\Delta x}\lambda \quad (4)$$

The penetration depth λ, increases by a factor of 10 for every two decades of decreasing frequency. From Fig. 4, the temperature rise ΔT_h of the heater is about 1.6 K in the maximum heatflow case. The sample thickness is 7 mm, which yields $\Delta T_{sa}/\Delta x = 2.3\ \mathrm{K\ mm^{-1}}$ in the worst case. At $\omega = 3.98\times 2\pi\ \mathrm{rads^{-1}}$, the penetration depth of the sample is about 0.03 mm. As a result from Eq. (4), this yields a correction to the sample temperature: $(\Delta T_{sa}/\Delta x)\lambda < -0.01$ K. The correction increases to about -0.14 K at $\omega = 0.01\times 2\pi\ \mathrm{rads^{-1}}$. For the low heatflow case the corresponding corrections are; -0.003 K and -0.04 K, respectively. Measurements of the shift in the SmA/N transition temperature for different frequencies would yield a more precise determination of the correction to the sample temperature due to the temperature gradient in the sample, but this was not done here. The analysis presented here shows, however, that the temperature gradient in the sample causes only a small shift in the temperature (<0.1 K) from that of the heater. As a consequence, a calibration done at constant frequency can be used at all frequencies with an increased error of less than about 0.1 K.

To minimise the effect of the dc-heating, it is favourable to use a low heater power. This is in conflict with the demand of the lock-in amplifier to obtain a sufficiently large signal to phase-lock the 3ω-signal. Since $U_{3\omega} \propto U_0^3$ a decrease of the bridge driving voltage ($2U_0$), rapidly leads to a situation where the 3ω-signal is below the noise level of the measuring system. The $\kappa c_p|^{\Phi_{lo}}$ results in Fig. 3 are measured using a heater power which yields a sufficiently large 3ω-signal, and the peakwidth is about 0.5 K. The behaviour above and below the peak is different compared to the $\kappa c_p|^{\Phi_{hi}}$ result which has flat regions below and above the transition temperature. A possible explanation for the differences could be that the Φ_{hi} result is influenced by the thermal conductivity contribution above and below the peak due to the temperature averaging mechanism (a large averaging window). Using a photoacoustic method, Thoen and Glorieux [10] measured κ and c_p of the liquid crystal 8CB (octylcyanobiphenyl). The results are similar to those for 8OCB, i.e. there is a SmA/N transition at 306 K. Both below and above the SmA/N transition, the thermal conductivity κ is decreasing linearly with temperature. Thus, since c_p is increasing the results of the product κc_p will be flattened above and below the peak. The Φ_{hi} results show a significantly suppressed and broadened peakwidth of about 2 K, in comparison with the Φ_{lo} results which has a peakwidth of only 0.5 K. This difference can be explained by a temperature gradient in the heater.

If there is a temperature gradient in the heater, the measured value will be an average over the temperature interval ΔT_{grad}. To correctly show how the averaging process works one would have to know the exact distribution of temperatures in the plane of the heater. A simplified model of the temperature distribution would be that the response from every temperature in the interval ΔT_{grad} is equally represented in the measured signal, i.e. a dual-ramp shaped gradient of height ΔT_{grad} along the heater. To test this hypothesis, the results for $\kappa c_p|^{\Phi_{lo}}$ were averaged using this simplified model and compared to the results for $\kappa c_p|^{\Phi_{hi}}$. The

averages were calculated using a running average with a window of ΔT_{grad}=1.2 K. This temperature gradient corresponds to the difference between the Φ_{hi} transition temperature and that for Φ_{lo}. If one consider the difference above and below the peak, described above, by subtracting a baseline from $\kappa c_p|^{\Phi_{lo}}$, then the simple averaging procedure of the $\kappa c_p|^{\Phi_{lo}}$ results yields a broadened peak with a width of about 2 K, which is in good agreement with the $\kappa c_p|^{\Phi_{hi}}$ results. This indicates that the simple model can be used to understand the results when measuring with high heatflow. The simplified model also shows that the peak maximum of κ c_p should decrease as a result of the gradient, which is in good agreement with the experimental results.

4. Conclusions

Heat capacity spectrometers based on the 3ω-method have an inherent complication as the alternating electric current, through dc-heating, rises the temperature of the heater above the ambient temperature. Moreover, for higher heater powers, a temperature difference ΔT_{grad} is created along the heater. The temperature rise ΔT_h, of the heater also generates a gradient through the sample. The temperature scale will be influenced by the temperature rise so that a measured κ c_p value, at temperature T_{amp} measured by thermocouples T1 and T3 (see Fig. 1), will appear at a lower temperature than expected. The measurement of the SmA/N transition shows that the temperature rise is proportional to the power input to the heater. Therefore, the temperature scale can be corrected: $T_{corr}=T_{amb}+\Delta T_h$, where $\Delta T_h=55.2P$ and P is the electrical power input to the heater.

The correction of the sample temperature due to the temperature gradient in the 8OCB sample is small compared to ΔT_h. For the high heatflow case, the correction of the sample temperature is <-0.01 K at $\omega=3.98\times 2\pi$ rads^{-1}. The correction increases to about -0.14 K at $\omega=0.01\times 2\pi$ rads^{-1}. For the low heatflow case the corresponding corrections are; -0.003 K and -0.04 K, respectively.

Due to the temperature gradient ΔT_{grad}, the area in the middle of the heater gets hotter than the peripheral parts where the electrical contacts are placed. As a consequence, the result for κ c_p corresponds to an average in this temperature interval. The peak in κ c_p associated with the SmA/N transition of the liquid crystal 8OCB is broadened by the averaging process and the peak-value is suppressed. A peak of width 0.5 K for P=7.7 mW will be broadened to 2 K for P=29.4 mW.

Acknowledgements

We thank Prof. C. Schick for valuable comments and for suggesting the liquid crystal octyloxycyanobiphenyl (8OCB) as a suitable compound for temperature calibration of the 3ω-dynamic heat capacity spectrometer. This work was supported by EU INCO COPERNICUS project IC15CT96-0821.

References

[1] N.O. Birge, S.R. Nagel, Phys. Rev. Lett. 54 (1985) 2674.
[2] N.O. Birge, S.R. Nagel, Rev. Sci. Instrum. 58 (1987) 1464.
[3] U.G. Jonsson, O. Andersson, Meas. Sci. Technol. 9 (1998) 1873.
[4] U.G. Jonsson, Lic. thesis (1999).
[5] J.D. LeGrange, J.M. Mochel, Phys. Rev. A 23 (1980) 3215.
[6] C.W. Garland, G.B. Kasting, K.J. Lushington, Phys. Rev. Lett. 43 (1979) 1420.
[7] G.W.H. Höhne, J. Schawe, C. Schick, Thermochim. Acta 221 (1993) 129.
[8] A. Zywocinski, S.A. Wieczorek, J. Stecki, Phys. Rev. A 36 (1987) 1901.
[9] D.L. Johnson, C.F. Hayes, R.J. deHoff, C.A. Schantz, Phys. Rev. B 18 (1978) 4902.
[10] J. Thoen, C. Glorieux, Thermochim. Acta 304/305 (1997) 141.